Dynamic response of a quantum wire structure

Yabin Yu,[1] T. C. Au Yeung,[2] and W. Z. Shangguan[2]
[1]*The Hong Kong Polytechnic University, Department of Building Service Engineering, Hong Kong*
[2]*Nanyang Technological University, School of Electrical and Electronic Engineering, Singapore 639798*
(Received 17 July 2002; published 17 December 2002)

We present an investigation of the dynamical response for a quantum wire structure with reservoirs. The capacitance, admittance, and the distribution of internal potential and charge density are calculated. Our numerical calculation for internal potential and charge density shows that the induced charge density is mainly distributed in transition regions between the reservoirs and the wire, and that once any quantum channel opens, the potential drop is very sharp and occurs in the transition regions. Small Friedel oscillations in the charge density as well as charge peaks are observed. We show in our model that in the reservoirs the characteristic potentials tend to unity or zero. The results of capacitance and emittance show the resonant peaks due to the opening of an additional channel, and the oscillations are related to the longitudinal states of the quantum wire. For capacitance, a steplike behavior appears as the number of open channels increase, but for emittance such steplike structure is not observed. Furthermore, we found that the emittance curves may lie either below or above capacitance, so the charge transmission may give positive or negative contributions to the emittance.

DOI: 10.1103/PhysRevB.66.235315 PACS number(s): 73.23.Ad, 73.61.−r

I. INTRODUCTION

The transport properties of ballistic quantum systems have been extensively studied since the early 1980s. A typical system, the one-dimensional (1D) ballistic quantum wire (QW) connected to wide reservoirs, has attracted intensive research interest, both experimentally and theoretically, because of its fundamental importance and potential microelectronic applications. Studies of the dc and ac conductance of this structure have been frequently reported in the literature. An important issue is the effect of the Coulomb interaction between electrons on the conductance in the system. For the dc case, the commonly used Luttinger liquid model[1–6] for interacting electrons gives the renormalization of the conductance quantum obtained in noninteracting Fermi liquids, and the model could explain some experimental results. Thus, the Coulomb interaction makes a quantitative correction to the conductance of the system. For the time-dependent case, however, the interaction plays a key role in ensuring the charge (current) conservation and the gauge invariance under a potential shift.[7–10] Büttiker *et al*. have discussed this point extensively and formulated the theory of ac conductance in the linear response and low-frequency regime including the effects of charging, in the both frameworks of continuous and discrete internal potential models.[8–10] The effect of the interaction on the ac conductance of a QW with reservoirs was studied in Ref. 11 by using the random phase approximation. The internal potential and electron-density distribution in the system were investigated in Ref. 12 based on the Hartree-Fock approximation. Using the bosonization technique, Sablikov and Shchamkhalova[5] also studied ac electron transport in a QW with Coulomb interaction, and give the distribution of internal potential and electron density. Furthermore, the ac response in QW's of infinite length has been studied.[13,14] To our knowledge, however, the distribution of potential and charge density in the transition regions between the QW and the reservoirs has not been studied qualitatively. For the ballistic wire systems the variation of the potential in such regions is very important and would give rise to a dominant charge distribution of the systems. In fact, the results of Ref. 12 indicated that in the QW the potential drop and charge mainly appear near the contacts. In this paper we follow the scattering theory developed by Büttiker *et al.* to study the dynamical response of the QW system to a time-dependent voltage. We calculate the internal potential and charge density in the ballistic system including the transition regions, and present the results of capacitance and emittance.

II. MODEL AND FORMULA

The model that we consider in this paper is a 2D-1D-2D system (see Fig. 1), which includes a narrow ballistic channel, i.e., QW (C: $|x|<d$ and $|y|<a/2$), and two wide 2D electron reservoirs, i.e. the left (L: $x<-d$ and $|y|<W/2$) and right (R: $x>d$ and $|y|<W/2$) contacts. We will investigate the linear response of the system to a time-dependent external voltage. When voltage is applied to the reservoirs, besides the scattering processes for electrons in the 2D-

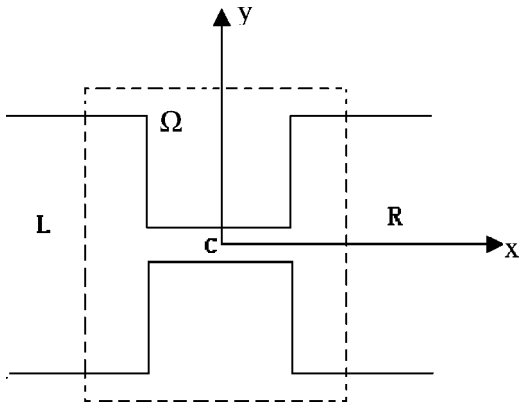

FIG. 1. Schematic view of a quantum ballistic wire structure with two reservoirs. Ω is a hypothetical volume, and it is assumed that no electric field lines penetrate the surface of Ω.

1D-2D system, we have to consider the piled-up charge and the induced internal electrostatic potential in the system, which affect the transport of the electrons. To proceed, we imagine a volume Ω (the dashed-line box in Fig. 1) that encloses the entire QW and parts of the reservoirs and is large enough to include all the electric field lines and charges of the system.

A. Internal potential and charge density

In the scattering theory of quantum transport for mesoscopic conductors developed by Büttiker *et al.*, the local partial density of states (LPDOS) and injectivities are two very important concepts. The LPDOS originates from the displacement current, which is the response of the long-range Coulomb interaction to ac perturbations, and is given by

$$\frac{dn_{\alpha\beta}(\mathbf{r})}{dE}=\frac{-1}{4\pi i}\int dE\left(\frac{-\partial f}{\partial E}\right)\mathrm{Tr}\left[s^{\dagger}_{\alpha\beta}\frac{\delta s_{\alpha\beta}}{\delta U(\mathbf{r})}-\frac{\delta s^{\dagger}_{\alpha\beta}}{\delta U(\mathbf{r})}s_{\alpha\beta}\right], \tag{1}$$

where α, β are the reservoir indices (here $\alpha=1$ or L for the left reservoir, and $\alpha=2$ or R for the right reservoir) and $s_{\alpha\beta}$ are the scattering matrices. With the LPDOS the injectivities are defined by

$$\frac{dn_{\alpha}(\mathbf{r})}{dE}=\sum_{\beta}\frac{dn_{\beta\alpha}(\mathbf{r})}{dE}. \tag{2}$$

The injectivity describes the carrier density of states incident in the reservoir α regardless of which reservoir it exits.[9] This is justified by the following formula of $dn_{\alpha}(x)/dE$ derived by Gasperian *et al.*:[15]

$$\frac{dn_{\alpha}(\mathbf{r})}{dE}=\int dE\left(\frac{-\partial f}{\partial E}\right)\frac{1}{hv_{\alpha}}|\psi(\mathbf{r})|^2, \tag{3}$$

where v_{α} is the incident velocity of the carriers into the reservoir α, and $\psi(\mathbf{r})$ the corresponding incoming wave function.

In order to calculate the dynamical response of the QW system, based on the theory of Büttiker *et al.*, we have to calculate the injectivities, $dn_{\alpha}(\mathbf{r})/dE$, and local density of states (LDOS), $dn(\mathbf{r})/dE=\Sigma_{\alpha}dn_{\alpha}(\mathbf{r})/dE$.[8,9,15,16] Because our interest is electron transport and the distribution of potential and charge density along the x axis, we need to integrate the injectivities and the density of states over the transverse direction (i.e., the y direction): $dn_{\alpha}(x)/dE=\int[dn_{\alpha}(\mathbf{r})/dE]dy$ and $dn(x)/dE=\int[dn(\mathbf{r})/dE]dy$. We first calculate the electron wave functions incident from the left, using the mode-matching approach.[17] In the left (L) and right (R) reservoirs the wave functions can be read as

$$\Psi^{L}_{l}(x,y)=\sum_{l'}\{\delta_{l'l}e^{ik^{x}_{l}x}+S_{11,l'l}e^{-ik^{x}_{l'}x}\}\phi^{W}_{l'}(y)\ \text{ for }\ x<-d, \tag{4}$$

$$\Psi^{R}_{l}(x,y)=\sum_{l'}S_{21,l'l}e^{ik^{x}_{l'}x}\phi^{W}_{l'}(y)\quad \text{for}\ x>d, \tag{5}$$

where $\phi^{W}_{l'}(y)$ are the transverse eigenfunctions in the reservoirs, $k^{x}_{l}=[2m^{*}E/\hbar-(l\pi/W)^2]^{1/2}$ the incident wave vectors in the x direction, m^{*} the effective mass of electrons, and E the incident energy of the electron. The sum in Eq. (4) is taken over all transverse components l', and $k^{x}_{l'}$ in Eq. (4) can be either real or imaginary, i.e., evanescent waves are included. In the QW, the wave functions may be expressed as

$$\Psi^{C}_{l}(x,y)=\sum_{m}[A_{ml}e^{ik^{x}_{m}x}+B_{ml}e^{-ik^{x}_{m}x}]\phi^{C}_{m}(y), \tag{6}$$

where $\phi^{C}_{m}(y)$ are the transverse eigenfunctions of electrons in the QW, $k^{x}_{m}=[2m^{*}E/\hbar-(m\pi/a)^2]^{1/2}$, and the sum is again taken over all channels m including all evanescent and transport wave functions.

The continuity of Ψ_l and $\partial\Psi_l/\partial x$ at $x=-d$ and d yields

$$\sum_{n}[(T_{mn}+k^{x}_{n}\delta_{mn})e^{-ik^{x}_{n}d}A_{nl}+(T_{mn}-k^{x}_{n}\delta_{mn})e^{ik^{x}_{n}d}B_{nl}], \tag{7}$$

$$\sum_{n}[(T_{mn}-k^{x}_{n}\delta_{mn})e^{ik^{x}_{n}d}A_{nl}+(T_{mn}+k^{x}_{n}\delta_{mn})e^{-ik^{x}_{n}d}B_{nl}], \tag{8}$$

and

$$S_{11,l'l}=-\delta_{l'l}e^{-i(k^{x}_{l'}+k^{x}_{l})d}+\sum_{n}M_{l'n}(A_{ml}e^{-i(k^{x}_{m}+k^{x}_{l'})d}+B_{ml}e^{i(k^{x}_{m}-k^{x}_{l'})d}), \tag{9}$$

$$S_{21,l'l}=\sum_{n}M_{l'n}(A_{ml}e^{i(k^{x}_{m}-k^{x}_{l'})d}+B_{ml}e^{-i(k^{x}_{m}+k^{x}_{l'})d}), \tag{10}$$

where $M_{l'n}=\int[\phi^{W}_{l'}(y)]^{*}\phi^{C}_{n}(y)dy$ and $T_{mn}=\Sigma_{l'}k^{x}_{l'}(M_{l'm})^{*}M_{l'n}$. Furthermore, the elements of the scattering matrix can be obtained by the following formula:

$$\mathbf{s}_{\alpha\beta,l'l}(E)=\left(\frac{v_{l'}}{v_{l}}\right)^{1/2}S_{\sigma\beta,l'l}(E)\quad \text{for values of } l' \text{ that give real } k^{x}_{l'}, \tag{11}$$

where $v_l=\hbar k^{x}_{l}/m^{*}$ ($v_{l'}=\hbar k^{x}_{l'}/m^{*}$) is the incident (emergent) velocity of the electrons in the direction of transport (x axis). Combining Eqs. (4)–(11), we obtain first the wave function of the electrons in the system, and then the injectivity[15]

$$\frac{dn_{L}(x)}{dE}=\sum_{l}\int dE\left(\frac{-\partial f}{\partial E}\right)\int dy\frac{1}{hv_{l}}|\psi_{l}(x,y)|^2. \tag{12}$$

For our symmetrical system,

$$\frac{dn_{R}(x)}{dE}=\frac{dn_{L}(-x)}{dE}. \tag{13}$$

The LDOS is then given by

$$\frac{dn(x)}{dE}=\frac{dn_L(x)}{dE}+\frac{dn_R(x)}{dE}. \tag{14}$$

In the presence of a small and low-frequency ac voltage $v_{\rm ac}$ applied to the reservoir α ($\alpha=1$ or 2), the internal potential $U(x)$ is given by $U(x)=u_\alpha(x)v_{\rm ac}$, where u_α is called the characteristic function. Using the Thomas-Fermi approximation, the characteristic potential function u_α is governed by the Poisson equation:[9,16]

$$-\nabla^2 u_\alpha+\frac{e^2}{\varepsilon_0}\frac{dn(\mathbf{r})}{dE}u_\alpha(x)=\frac{e^2}{\varepsilon_0}\frac{dn_\alpha(\mathbf{r})}{dE},\quad \alpha=1,2. \tag{15}$$

Under the Thomas-Fermi approximation the second term in Eq. (15) is the induced charges in the conductor and the third term is clearly the injected charges. Here we neglect the variation of the potential in the transverse direction, and assume that the characteristic function is a function of x only. We obtain the following equation by integrating over the transverse direction:

$$-\frac{d^2u_\alpha(x)}{dx^2}+\frac{e^2}{\varepsilon_0 A(x)}\frac{dn(x)}{dE}u_\alpha(x)=\frac{e^2}{\varepsilon_0 A(x)}\frac{dn_\alpha(x)}{dE} \tag{16}$$

where $A(x)$ represents the cross-sectional area of the QW and reservoirs. In the QW $A=ab$, and in the reservoirs $A=Wb$, where b is the thickness of the QW structure.

To solve Eq. (16) for $u_\alpha(x)$, we need the boundary values of $u_\alpha(x)$. Here we use the neutrality condition[18] to determine the boundary values of $u_\alpha(x)$:

$$u_\alpha(x_L)=\frac{dn_\alpha(x_L)}{dE}\Big/\frac{dn(x_L)}{dE},$$

$$u_\alpha(x_R)=\frac{dn_\alpha(x_R)}{dE}\Big/\frac{dn(x_R)}{dE}, \tag{17}$$

where x_L and x_R are left and right boundary lines of the region Ω (see Fig. 1), which is a hypothetical volume[8–10,19] and is so large that electric field lines through the surface of it vanish, i.e., the electric field is completely screened within the volume. If the reservoir is very large (the width W is infinite), we can see from Eq. (17) that the characteristic potentials $u_1(x_L)$ $[u_2(x_R)]$ and $u_1(x_R)$ $[u_2(x_L)]$ are unity and zero, respectively. In our case, they are close to unity or zero. From Eq. (16), we know that when the system is biased by a small voltage δV applied to reservoir α, the distribution of the charge density in Ω is given by $\delta q(x)=\rho(x)\delta V$, and

$$\rho(x)=\frac{dq(x)}{dV}=-\varepsilon_0 A(x)\frac{d^2u_\alpha(x)}{dx^2}$$

$$=e^2\left[\frac{dn_\alpha(x)}{dE}-\frac{dn(x)}{dE}u_\alpha(x)\right]. \tag{18}$$

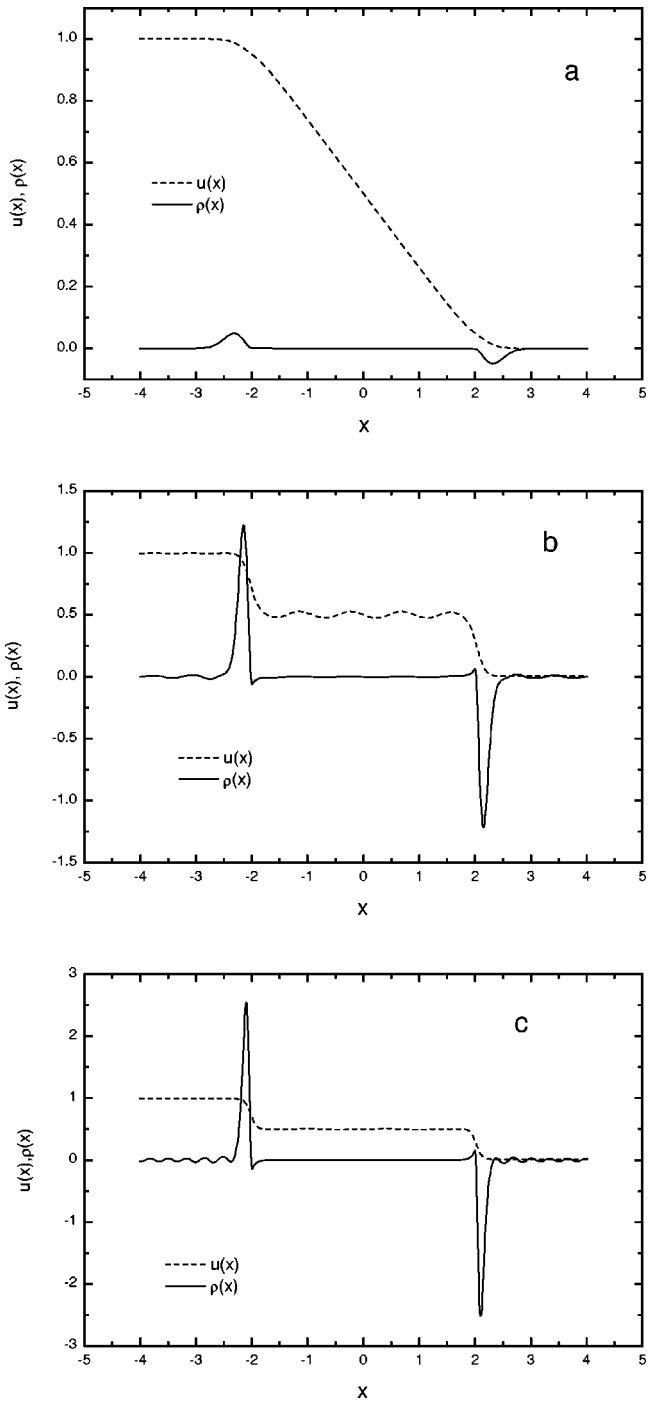

FIG. 2. Distribution of internal potential and charge density for (a) $\mu=0.1$, (b) $\mu=2.2$, and (c) $\mu=9.5$. Other parameters are $b=0.5$, $d=2$, and $W=50$. The energy is in units of the ground energy Δ, and length in units of the QW length a (=50 nm).

B. Capacitance and low-frequency admittance

According to Eq. (18), when a small voltage δV is applied to the left reservoir the total charge in the left half portion of Ω is given by

$$\delta Q=\int_{x_L}^{0}\delta q(x)dx,$$

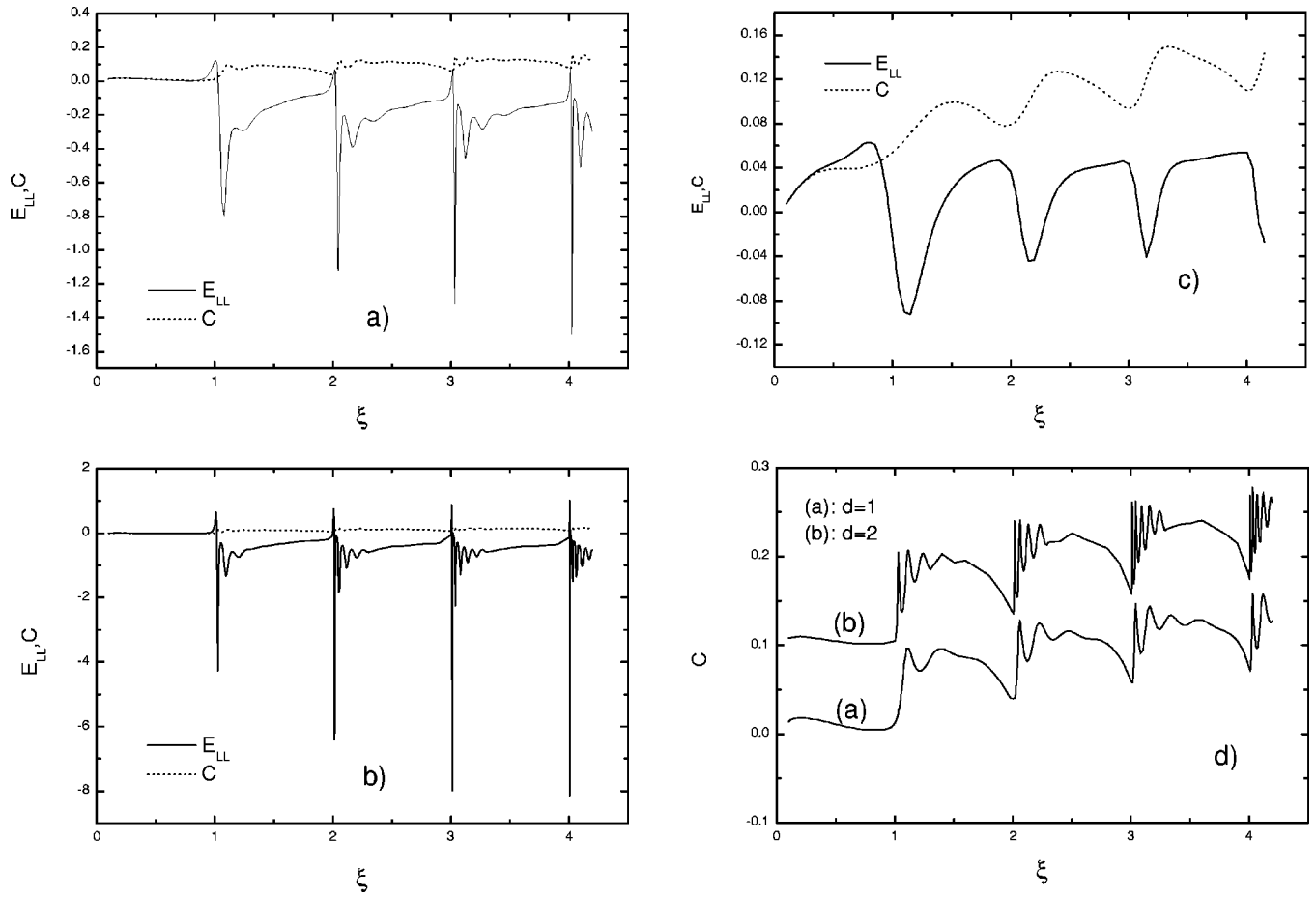

FIG. 3. The plots of emittance and capacitance as functions of chemical potential μ, for QW length (a) $2d=2$, (b) $2d=4$, and (c) $2d=0.6$. (d) is a replotting of the capacitance in (a) and (b). The other parameters are $b=0.5$ and $W=20$. The energy is in units of the ground energy Δ, and length in units of QW length a (=50 nm).

and then the capacitance of the QW system can be calculated by the following:

$$C=\frac{\delta Q}{\delta V}=\int_{x_L}^{0}\rho(x)dx=e^2\int_{x_L}^{0}\left[\frac{dn_L(x)}{dE}-\frac{dn(x)}{dE}u_L(x)\right]dx. \tag{19}$$

With the quantities of the partial density of states (PDOS), injectivities, and internal potentials obtained, we can calculate the admittance for low frequencies:[8–10,19]

$$g_{\alpha\beta}(\omega)=g_{\alpha\beta}(0)-i\omega e^2E_{\alpha\beta}, \tag{20}$$

where ω is the frequency of the ac bias, $g_{\alpha\beta}(0)$ the dc conductance, and

$$E_{\alpha\beta}=e^2\frac{dN_{\alpha\beta}}{dE}-e^2\int dx\frac{dn_\alpha(x)}{dE}u_\beta(x) \tag{21}$$

is the emittance. In the first term of Eq. (21),

$$\frac{dN_{\alpha\beta}}{dE}=\frac{1}{4\pi i}\int dE\left(\frac{-\partial f}{\partial E}\right)\mathrm{Tr}\left[\mathbf{s}_{\alpha\beta}^{\dagger}\frac{d\mathbf{s}_{\alpha\beta}}{dE}-\frac{d\mathbf{s}_{\alpha\beta}^{\dagger}}{dE}\mathbf{s}_{\alpha\beta}\right] \tag{22}$$

are the partial densities of states, and may be interpreted as the carrier density of states in volume Ω, which consists of those carriers injected from reservoir β and emerging from reservoir α. Equation (22) is exact only when Ω is infinite, i.e., $|x_L|\to\infty$.[20] For the finite-size system, PDOS can be defined as[8–10,19]

$$\frac{dN_{\alpha\beta}}{dE}=\int_{x_L}^{x_R}\frac{dn_{\alpha\beta}(x)}{dE}dx, \tag{23}$$

where

$$\frac{dn_{\alpha\beta}(x)}{dE}=\frac{-1}{4\pi i}\int dE\left(\frac{-\partial f}{\partial E}\right)\mathrm{Tr}\left[\mathbf{s}_{\alpha\beta}^{\dagger}\frac{\delta\mathbf{s}_{\alpha\beta}}{\delta U(x)}-\frac{\delta\mathbf{s}_{\alpha\beta}^{\dagger}}{\delta U(x)}\mathbf{s}_{\alpha\beta}\right] \tag{24}$$

are the one-dimensional LPDOS. $\delta\mathbf{s}_{\alpha\beta}/\delta U(x)$ is the functional derivative of $\mathbf{s}_{\alpha\beta}(E,U(x))$, and in our case it is taken around $U(x)=0$. Equations (23) and (24) indicate that $d\mathbf{s}_{\alpha\beta}/dE$ in the PDOS (22) should be replaced by $-d\mathbf{s}_{\alpha\beta}/dU=-\int_{x_L}^{x_R}[\delta\mathbf{s}_{\alpha\beta}/\delta U(x)]dx$. We can calculate $d\mathbf{s}_{\alpha\beta}/dU$ as follows. In the considered region Ω, introducing a constant potential U, we repeat the above process of calculating wave functions, and get the scattering matrix

$\mathbf{s}_{\alpha\beta}(E,U)$. Alternatively, we can set the electron "energy" as E' and E in and out of the region Ω, respectively, and get $\mathbf{s}_{\alpha\beta}(E,E')$. We then have

$$-\frac{d\mathbf{s}_{\alpha\beta}}{dU}=-\int_{x_L}^{x_R}\frac{\delta\mathbf{s}_{\alpha\beta}}{\delta U(x)}dx=-\left.\frac{d\mathbf{s}_{\alpha\beta}(E,U)}{dU}\right|_{U=0}$$

$$=\left.\frac{d\mathbf{s}_{\alpha\beta}(E,E')}{dE'}\right|_{E'=E}. \tag{25}$$

III. NUMERICAL RESULTS

In this section, we first study the internal potential $u(x)$ and the charge density $\rho(x)$ with various Fermi levels μ $(=\mu_L=\mu_R)$ for temperatures $T=0$, and then present the numerical results of ac conductance and capacitance. As aforementioned we use $\Delta=h^2/8m^*a^2$, the transverse ground state energy of the QW, as the unit of energy, and the QW width a as the unit of distance. To solve the Poisson equation (16), we set $a=50$ nm, and the thickness of the QW structure $b=a/2$. In our calculation, we take $x_L=-x_R$.

In Fig. 2 we present plots of $u_L(x)$ and $\rho(x)$ for Fermi energies $\mu=0.1$ [Fig. 2(a)], 2.2 [Fig. 2(b)], and $\mu=9.5$ [Fig. 2(c)]. Figure 2(a) corresponds to the case in which the Fermi energy is smaller than the transverse ground energy (Δ) of the QW. In this case, the transverse ground state energy plays the role of a potential barrier for the incident electrons, so what we see is the behavior of single barrier tunneling, and the QW system is a barrier capacitor. The shape of $u(x)$ is a smooth curve and almost linear inside the QW, and the potential drop is uniform between the two ends of Ω. In the case of $\mu>\Delta$, however, Figs. 2(b) and 2(c) show that the abrupt drops in the potential appear within the transition regions between the QW and the reservoirs. For all curves [Fig. 2(a), 2(b), and 2(c)], we see that $u(x)\approx 1(0)$ on the left (right) side of the considered volume Ω, and that the charge distribution $\rho(x)$ is considerable only around the left and right ends of the QW and otherwise almost zero. It is noticed that in the QW the charge distribution is almost zero, but the variation of the internal potential does not vanish [see Figs. 2(a) and 2(b)]. It is not surprising: this is because the one-dimensional charge distribution is given by integrating over the cross-sectional area of the system, and the cross-sectional area of contact is much larger than that of the QW. In addition to the two peaks of charge distribution on the two sides of the QW, the Friedel oscillations in the charge densities are also observed in the reservoir and the QW, but much smaller than the charge peaks.

While the distribution of the internal potential and charge density reveals information about the system under investigation, the capacitance and ac conductance of the QW device may present a result that is directly capable of being verified with experimental data. Below we calculate the capacitance and emittance at zero temperature using Eqs. (19) and (21). In Fig. 3 we present the capacitance C and diagonal emittance E_{11} as functions of the chemical potential, for the QW length $2d=2$ [Fig. 2(a)] 4 [Fig. 2(b)] and contact width $W=20$, where the chemical potential is parametrized by ξ $=(\mu/\Delta)^{1/2}$. The emittance shows a positive and a negative resonant peak around the integral values of ξ, which corresponds to the stepjump of the dc conductance of the QW structures and is caused by the opening of additional quantum channels in the QW. This is a resonance related to the transverse energy levels of the QW. In addition to this resonance there is another type of resonance related to the longitudinal motion of electrons in the QW. The emittance and capacitance are oscillatory between the two neighboring resonances, corresponding to the opening of the next higher channel, and the strength and frequency of oscillation increase with the increase of chemical potential and the QW length. This oscillation is caused by longitudinal resonant electron states that occur when the length of the QW is approximately equal to integer multiples of half longitudinal Fermi wavelength,[17] i.e., $2d\approx k\lambda_F/2=\frac{1}{2}kh/\sqrt{2m^*(\mu-n^2\Delta)}$ $(k=1,2,3,\ldots;\quad n=1,2,3,\ldots)$. Furthermore, to get a clearer view, we plot the two capacitance curves of Figs. 3(a) and 3(b) in Fig. 3(d), where the

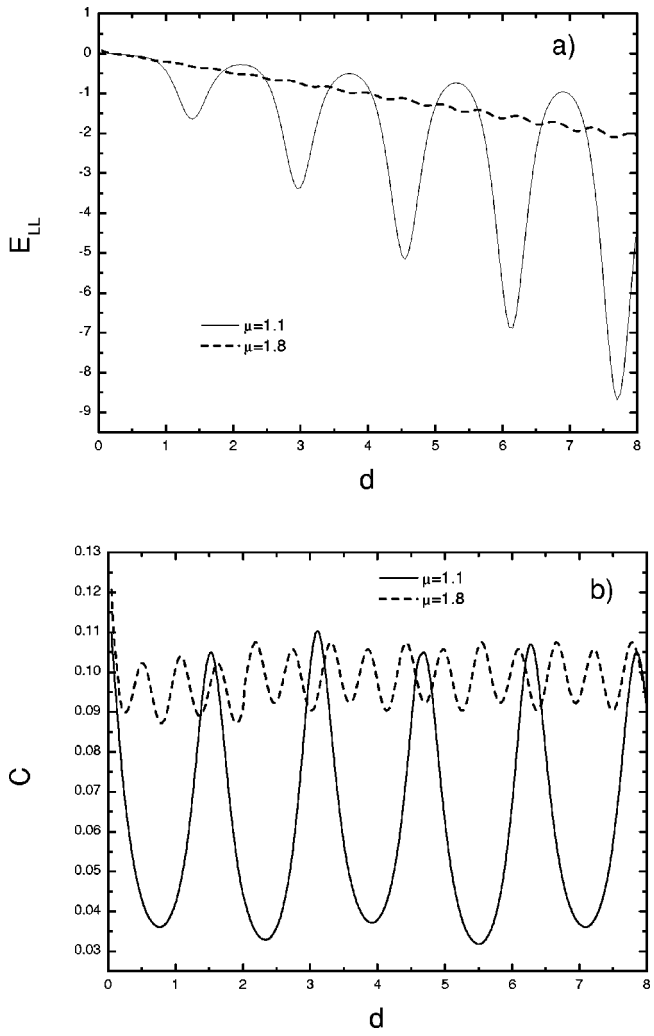

FIG. 4. The plots of emittance and capacitance as functions of QW length d for chemical potential $\mu=1.1$ and 1.8. The other parameters are the same as in Fig. 3. The energy is in units of the ground energy Δ, the emittance and capacitance in e^2/Δ, and length in units of QW length a $(=50$ nm).

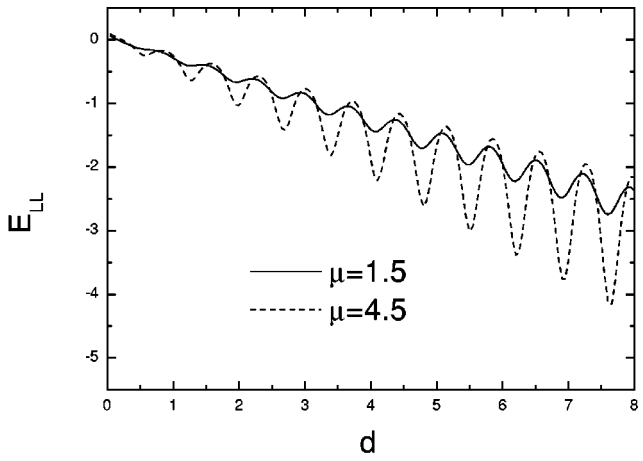

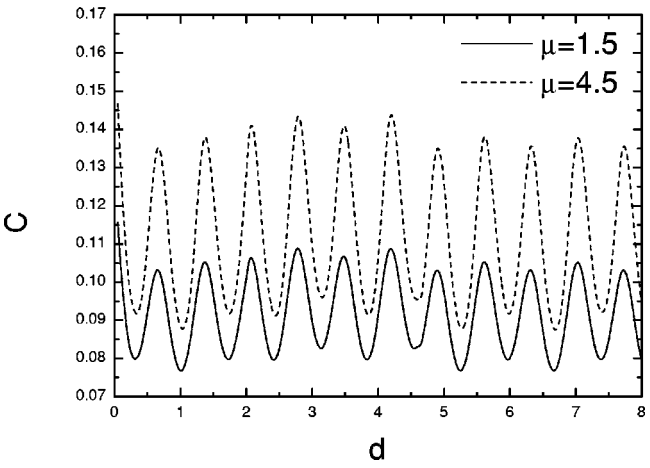

FIG. 5. The plots of emittance and capacitance as functions of QW length d for chemical potential $\mu=1.5$ and 4.5. The other parameters are the same as in Fig. 3. The energy is in units of the ground energy Δ, the emittance and capacitance in e^2/Δ, and length in units of QW length a ($=50$ nm).

curve for $d=1$ is offset vertically by 0.1 for a clearer comparison. In this figure, a steplike behavior is shown as the number of open channels increase, and the oscillation between the steps appears clearly. For emittance curves, the jump in value appears when the incident energy μ nears to the next higher transverse energy levels as mentioned above, but there is no steplike structure compared to capacitance curves. It is worth pointing out that in contrast to the results for a quantum point contact in Ref. 21, our results show that the emittance curves do not always lies below the capacitance curves, and when the Fermi energy is around and close to a transverse energy level of the QW the emittance gives a positive peak, and its value may be larger than the capacitance. So, in this case, the charge transmission would give a positive contribution to the emittance. In addition, this phenomena is QW-length dependent, and for a QW of very short length, unless the Fermi energy is close to and smaller than the ground energy Δ, the emittance always lies below the capacitance [see Fig. 3(c)].

In order to exhibit the resonance related to the longitudinal motion of electrons in the QW, more clearly, we present in Figs. 4–6 the emittance and capacitance as functions of the QW length d. As mentioned above, longitudinal resonance appears when $2d \approx k\lambda_F/2$. In the figures both curves of emittance and capacitance show a periodic oscillation with d, and the period is about $\frac{1}{2}h[8m^*(\mu-n^2\Delta)]^{-1/2}$. So we see that for the same value of n the oscillation frequency increases but the oscillation amplitude decreases with Fermi energy (see Fig. 4). For different values of n and μ, as long as the difference $\mu-n^2\Delta$ is same, the oscillation frequency would be the same (see Fig. 5). As for the case of $\mu<\Delta$, the oscillation feature disappears (see Fig. 6).

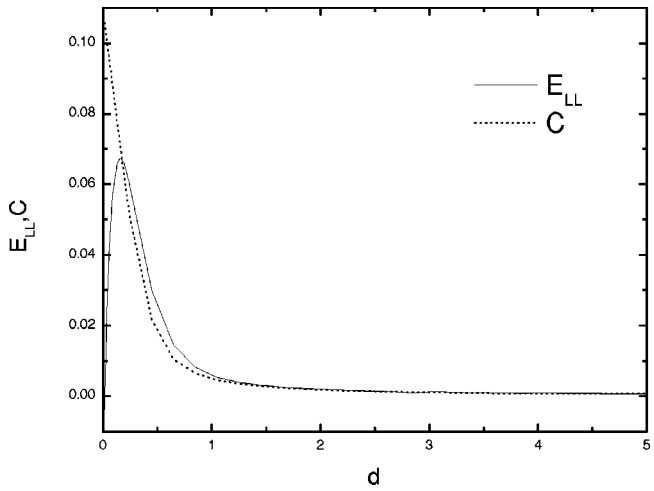

FIG. 6. The plots of emittance and capacitance as functions of QW length d for chemical potential $\mu=0.8$. The other parameters are the same as in Fig. 3. The energy is in units of the ground energy Δ, the emittance and capacitance in e^2/Δ, and length in units of QW length a ($=50$ nm).

IV. CONCLUSION

In conclusion, by employing the scattering theory developed by Büttiker *et al.* within a continuous model, we have studied the dynamical response of the QW system in which the QW and two-contact reservoirs are included. We have presented the calculation of various physics quantities such as the distribution of the internal potential and charge density, capacitance, and low-frequency ac conductance. Our numerical calculation for the internal potential and charge density shows that the induced charge density is mainly distributed in the transition regions between the reservoirs and the wire and antisymmetric about the QW center.

In our model we showed that in large reservoirs the characteristic potentials would tend to unity or zero. The potential drop in the transition region is very sharp and it happens when the Fermi energy is above the transverse ground state energy. Friedel oscillations in the charge density are observed in the QW system as well as charge peaks. For the results of capacitance and emittance, we oberved resonant peaks due to the opening of the next higher quantum channels and the oscillations related to the longitudinal resonant electron states of the QW. For the capacitance, steplike behavior appears as the number of open channels increase, but

the emittance curves do not have a steplike structure. Furthermore, we found that the emittance curves may lie below or above capacitance curves, and when the Fermi energy is around and close to a transverse energy level of the QW the emittance shows a peak, and its value may be larger than the capacitance. So, we conclude that the charge transmission may give positive or negative contributions to the emittance.

ACKNOWLEDGMENT

The first author would like to thank Professor W. K. Chow at the Hong Kong University for partly supporting this work.

[1] F. D. M. Haldane, J. Phys. C **14**, 2585 (1981); W. Apel and T. M. Rice, Phys. Rev. B **26**, 7063 (1982).
[2] C. L. Kane and M. P. A. Fisher, Phys. Rev. B **46**, 15 233 (1992).
[3] M. Ogata and H. Fukuyama, Phys. Rev. Lett. **73**, 468 (1994).
[4] D. L. Maslov and M. Stone, Phys. Rev. B **52**, R5539 (1995); V. V. Ponomarenko, *ibid.* **52**, R8666 (1995); I. Safi and H. J. Schulz, *ibid.* **52**, R17 040 (1995).
[5] V. A. Sablikov and B. S. Shchamkhalova, Phys. Rev. B **58**, 13 847 (1998).
[6] Siddhartha Lal, Sumathi Rao, and Diptiman Sen, Phys. Rev. Lett. **87**, 026801 (2001).
[7] R. Landauer, Phys. Scr., T **42**, 110 (1992).
[8] M. Büttiker, H. Thomas, and A. Prêtre, Z. Phys. B: Condens. Matter **94**, 133 (1994).
[9] M. Büttiker, J. Phys.: Condens. Matter **5**, 9361 (1993).
[10] M. Büttiker, A. Pretre, and H. Thomas, Phys. Rev. Lett. **70**, 4114 (1993); A. Prêtre, H. Thomas, and M. Büttiker, Phys. Rev. B **54**, 8130 (1996).
[11] Y. M. Nlanter and M. Büttiker, Europhys. Lett. **42**, 535 (1998).
[12] V. A. Sablikov, S. V. Polyakov, and M. Büttiker, Phys. Rev. B **61**, 13 763 (2000).
[13] K. A. Matveev and L. I. Glazman, Physica B **189**, 266 (1993).
[14] G. Cuniberti, M. Sassetti, and B. Kramer, Phys. Rev. B **57**, 1515 (1998).
[15] V. Gasparian, T. Christen, and M. Büttiker, Phys. Rev. A **54**, 4022 (1996).
[16] M. Büttiker, J. Math. Phys. **37**, 4793 (1996).
[17] G. Kirczenow, Phys. Rev. B **39**, R10 452 (1989); H. Q. Xu, Phys. Rev. B **48**, 8878 (1993).
[18] Xuean Zhao and Yi-Xin Chen, Phys. Rev. B **64**, 085326 (2001).
[19] M. Büttiker and T. Christen, in *Quantum Transport in Semiconductor Submicron Structures*, edited by B. Kramer (Kluwer Academic, Dordrecht, 1996), pp. 263–291.
[20] Q. Zheng, J. Wang, and H. Guo, Phys. Rev. B **56**, 12 462 (1997).
[21] T. Christen and M. Büttiker, Phys. Rev. Lett. **77**, 143 (1996).